Structure change, layer sliding, and metallization in high-pressure MoS_2

Liliana Hromadová,[1,2] Roman Martoňák,[1,*] and Erio Tosatti[2,3]

[1]*Department of Experimental Physics, Comenius University, Mlynská Dolina F2, 842 48 Bratislava, Slovakia*

[2]*International School for Advanced Studies (SISSA) and CNR-IOM Democritos, Via Bonomea 265, I-34136 Trieste, Italy*

[3]*The Abdus Salam International Centre for Theoretical Physics (ICTP), Strada Costiera 11, I-34151 Trieste, Italy*

(Received 7 November 2012; published 22 April 2013)

Based on *ab initio* calculations and metadynamics simulations, we predict that the electronic gap of $2H$-MoS_2, a layered insulator, will close under pressures in excess of 25 to 35 GPa. In the same pressure range, simulations and enthalpy optimization predict a structural transition. Free mutual sliding of layers takes place at this transition, the original $2H_c$ stacking changing to a $2H_a$ stacking typical of $2H$-$NbSe_2$, an event explaining for the first time previously mysterious x-ray diffraction and Raman data. Phonon and electron phonon calculations suggest that pristine MoS_2 will remain semimetallic up to very high pressures and is thus unlikely to develop superconductivity as it does upon metal intercalation.

DOI: 10.1103/PhysRevB.87.144105 PACS number(s): 61.50.Ks, 71.30.+h, 71.15.Pd, 74.62.Fj

I. INTRODUCTION

Transition metal dichalcogenides MX_2, where M is a transition metal and X = S, Se, and Te, are layered materials displaying a variety of electronic behavior from insulating to charge-density-wave to metallic to superconducting, with a rich scenario of phase transitions as a function of external parameters. The intercalation of electron-donating atomic species between the weakly bonded MX_2 layers is facile, turning the insulators to metals which are interesting catalysts, and which also often superconduct at cryogenic temperatures. Perhaps the best known case in point is that of MoS_2, a semiconductor with an indirect electronic band gap of 1.29 eV (Ref. 1), which in its pristine state is well known as a lubricant,[2] and more recently as a potential photovoltaic[3] and single-layer transistor[4] material. MoS_2 metallizes under the intercalation of alkalis and alkaline earths,[5] achieving superconducting temperatures up to 6 K. It has very recently also been shown to superconduct at even higher temperatures upon electric double layer (EDL) field doping.[6,7]

High pressure provides, besides doping, another general route to transform insulators to metals. Recently it was shown that the bilayer sheet of MoS_2 undergoes semiconductor-metal transition upon vertical compressive pressure.[8] The possibility that bulk MoS_2 might metallize under pressure is suggested by a negative pressure coefficient of resistivity[9] indicating gap shrinking $dE_G/dP < 0$. Whether and how high pressure gap closing and metallization in bulk could be achieved is, however, an open question, also because x-ray diffraction[10] and Raman spectroscopy[11] data indicate a structural transition taking place between 20 and 30 GPa to another phase of unknown structure and properties. What is the structural transition, whether high pressure metallization and possibly other phenomena such as charge-density waves or superconductivity will eventually occur or not, and what could be the interplay among these structural and electronic phenomena in an initially insulating material, are all open questions of considerable interest, for which MoS_2 can play a prototypical role. We alternated and combined well-established first principles density functional theory (DFT) calculations and *ab initio* metadynamics (AIMtD) simulations[12,13] to predict and clarify the simultaneous evolution of the structural and electronic properties of pristine MoS_2 under pressure.

The paper is organized as follows. In the second section we describe our simulation methodology. In the third section we present our results concerning structure, metallization and superconductivity of MoS_2 and compare them to available high pressure experimental data. In the final section we summarize our findings and draw conclusions.

II. SIMULATIONS METHODS

AIMtD simulation—where the supercell parameters act as collective variables—is a powerful computational tool to discover new and competing solid phases.[14,15] For *ab initio* molecular dynamics and structural relaxations we employed the Vienna *ab initio* simulation package (VASP)[16] with standard scalar relativistic projector-augmented wave (PAW) pseudopotentials (no spin-orbit included)[17] and a cutoff of 340 eV. Molecular dynamics (MD) simulations were performed using a 72-atoms $2\sqrt{(3)} \times 2\sqrt{(3)}$ supercell and $2 \times 2 \times 2$ Monkhorst-Pack[18] (MP) k-point sampling grid. For structural relaxations we used the six-atoms unit cell and a $9 \times 9 \times 5$ MP grid. The electronic structure calculations and structural optimizations were independently conducted using a variety of exchange-correlation functionals: local density approximation (LDA), generalized gradient approximation (GGA) with Perdew-Burke-Ernzerhof (PBE) parametrization,[19] hybrid functionals Becke three-parameter Lee-Yang-Parr (B3LYP)[20,21] and Heyd-Scuseria-Ernzerhof (HSE06).[22] Van der Waals interactions were included in the Grimme approximation[23] in the initial calculations at zero pressure, where they made an important contribution to the interplanar attraction, but were subsequently removed at high pressures. It turned out that at pressures above 5 GPa, in a regime where interlayer interactions are repulsive, it is GGA with PBE potential and without van der Waals corrections that provides the pressure evolution of the lattice parameters closest to the experimental data.

III. RESULTS

Within the above approximation we carried out accurate total energy-based structural relaxations at increasing pressures, refining the properties of the phase(s) discovered with AIMtD

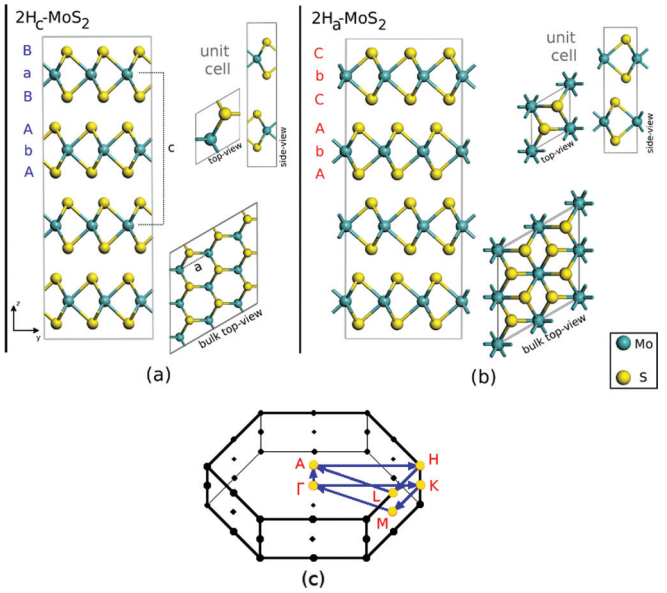

FIG. 1. (Color online) Structures of (a) $2H_c$-MoS_2 and (b) $2H_a$-MoS_2. (c) Brillouin zone for both structures (Ref. 24).

dynamical simulations. That combined approach produced the results which we now describe.

Static relaxation of the initial structure $2H_c$-MoS_2 (space group $P6_3/mmc$) of Fig. 1(a)[25] upon increasing pressure produced no instability towards other phases up to 50 GPa. The unit cell dimensions shrank anisotropically (Fig. 2) as expected from a softer c axis and harder a and b axes. The indirect electronic band gap also shrank as expected, and eventually closed near 25 GPa with an electron-hole wave vector $\vec{Q} \approx \frac{1}{2}(K - \Gamma)$ [Figs. 3(a) and 3(b)] where $K = (\frac{1}{3}, \frac{1}{3}, 0)$ is a Brillouin zone (BZ) edge point [Fig. 1(c)] thus predicting the band overlap metallization of $2H_c$-MoS_2 above 25 GPa. This result agrees with the very recent finding in Ref. 26. Alternative DFT calculations and relaxations carried out with the HSE06[22] and the B3LYP[20,21] approximations yielded a metallization pressure of 35 and 55 GPa, respectively. Since these approaches, especially the second one, are known to underestimate metallicity, whereas GGA/PBE may overestimate it, we conclude with good confidence that the pressure-induced gap closing of $2H_c$-MoS_2 should be placed between 25 and 35 GPa. At these pressures MoS_2 should therefore turn into a band overlap semimetal, reminiscent of other layered systems such as $1T$-$TiSe_2$ (Refs. 27,28). The Fermi surface of the $2H_c$-MoS_2 at 31 GPa is shown in Fig. 3(c) and contains a hole pocket at Γ and electron pockets at $\vec{Q}$.

Extending in this pressure region our calculations to the 72-atoms $2\sqrt{(3)} \times 2\sqrt{(3)}$ supercell in place of the initial six-atom unit cell, we further explored, in analogy with $TiSe_2$, the possible onset of a periodic lattice distortion or charge-density-wave phase (more properly called an "excitonic insulator"[29]). We performed structural optimizations of samples with small random displacements of atoms and looked for the possible onset of the accompanying periodic lattice distortion, but failed to find any. In fact, the possibility of an excitonic insulator driven superstructure with reciprocal lattice vector $\vec{Q}$ in the $2H_c$ structure in a narrow pressure interval near

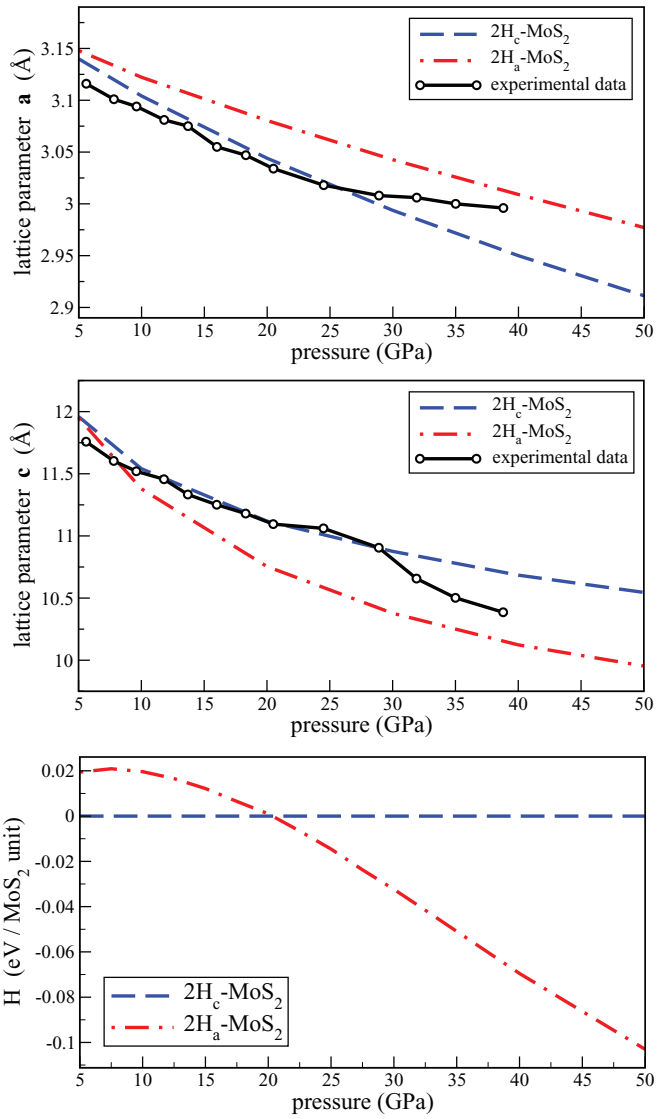

FIG. 2. (Color online) Calculated lattice parameters a (up) and c (middle), and relative enthalpies (bottom) of $2H_a$- and $2H_c$-MoS_2 structures as a function of pressure. The experimental data taken from Table I in Ref. 10 are in good agreement with calculated crossing of enthalpies at $p \sim 20$ GPa as shown in the bottom picture.

the insulator–semimetal transition, an occurrence which can be considered quite possible in MoS_2, cannot seriously be established within DFT. The search for excitonic insulators—exciton condensates accompanied either by a charge-density-wave-like periodic lattice distortion or by spin-density wave antiferromagnetism—requires a much more refined treatment of exchange beyond mean field. That treatment should be considered for the future in high pressure MoS_2 near gap closing. At the same time, careful experimental investigations would be desirable to detect any traces of charge or of spin superstructures in that pressure range.

However, the phase diagram of MoS_2 under pressure has more surprises in stock. We focused so far on the pressure evolution of the $2H_c$-MoS_2 initial structure. Actually, the local stability which we found upon relaxation is no guarantee for global stability at higher pressures. The AIMtD simulations, where the supercell vectors are biased away from the initial

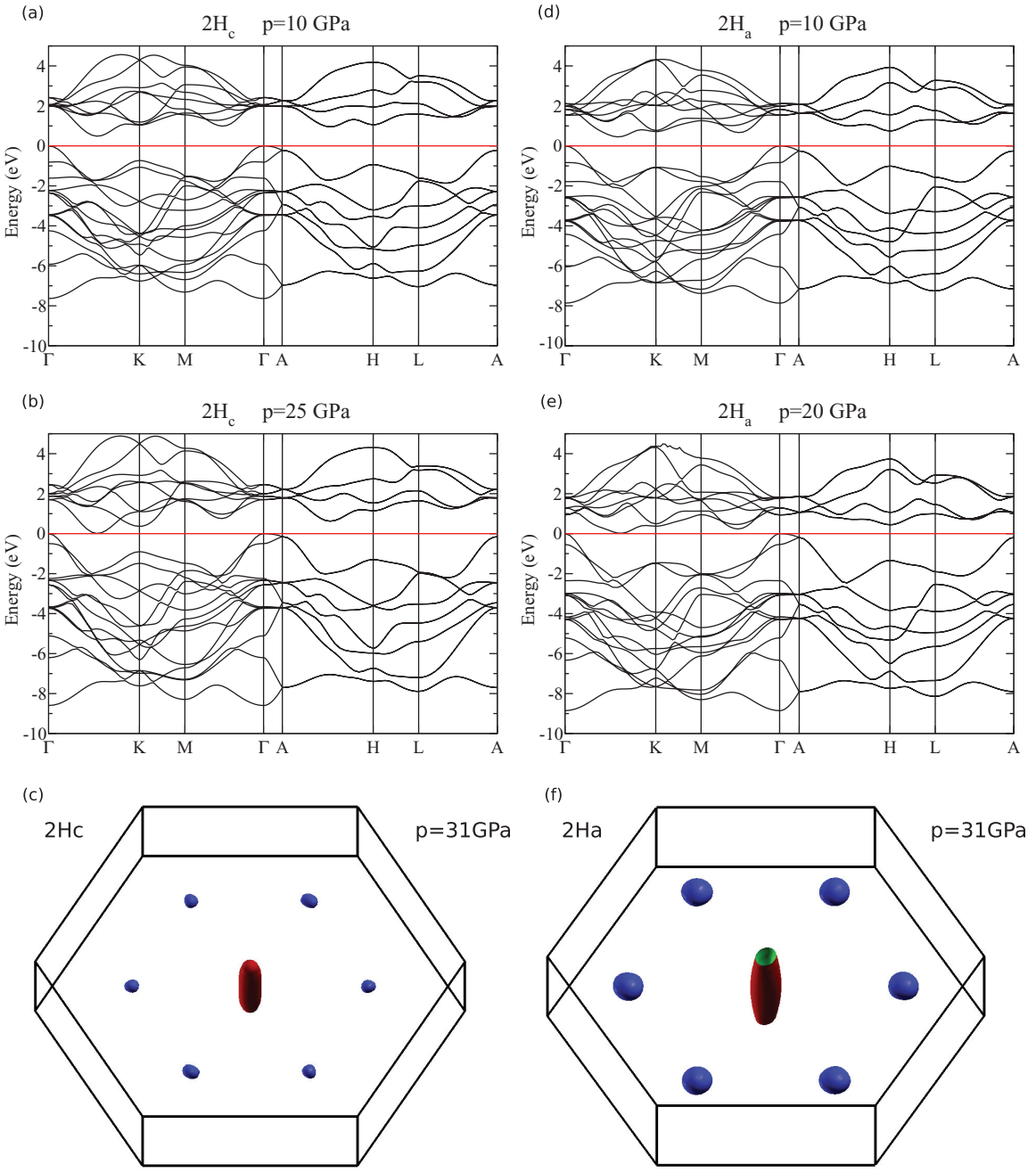

FIG. 3. (Color online) Calculated band structures of (a, b) $2H_c$- and (d, e) $2H_a$-MoS_2 at selected pressures. Fermi level is shown as red line. The bottom panels show the Fermi surface of the (c) $2H_c$- and (f) $2H_a$-MoS_2 structures at $p = 31$ GPa.

structure towards newer ones, can reveal the possible structures missed by straight relaxation. When applied to $2H_c$-MoS_2 in the 72-atom supercell at $p = 40$ GPa, it led to two successive and surprising sliding events shown in Fig. 4. In the first event after metastep 73 the two layers within the supercell shifted with respect to each other so that the Mo atom (x,y) coordinates in the two layers became coincident. At the same time the supercell developed a tilt: the α and β angles moved slightly away from right angle. In this intermediate structure the parameter a increased and the parameter c decreased from their original values. In the second event following metastep 125 the α and β angles returned to the original 90 degrees while the parameters a and c further increased and decreased, respectively. The final structure was relaxed at $p = 40$ GPa and $T = 0$ and was identified as $2H_a$—another $2H$ polytype with the same space group, but where the layer stacking is now AbA CbC in place of the initial AbA BaB stacking of $2H_c$ (Refs. 30,31). In the new structure—typical of, e.g., $2H$-$NbSe_2$—all Mo atoms share the same (x,y) coordinate positions. Thus the pressure-induced easy sliding of layers—a "superlubric" event, possibly even if not necessarily related to MoS_2's lubricant properties—transformed the $2H_c$ structure of MoS_2 to $2H_a$.

Through accurate structural relaxations and electronic structure calculations we refined the cell parameters, the enthalpy, and the electronic band structure of $2H_a$-MoS_2, with

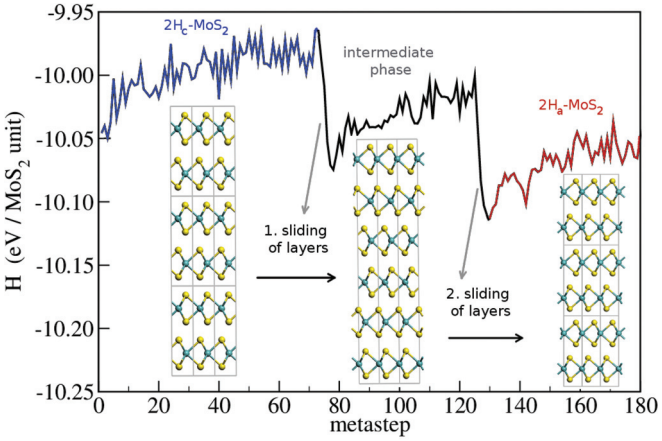

FIG. 4. (Color online) Evolution of enthalpy in the metadynamics simulation during transformation from $2H_c$-MoS_2 to $2H_a$-MoS_2 via an intermediate structure. Note the drop of enthalpy after each sliding event.

the results shown in Figs. 2 and 3. The $2H_c$ and $2H_a$ enthalpies cross near 20 GPa, justifying the structural transition discovered by AIMtD. Zero-point energy and entropic contributions for both phases were estimated within the quasiharmonic approximation at $p = 10$ GPa and $T = 300$ K. The difference between the two phases was smaller than 1 meV/atom and therefore these contributions were neglected in the figure. The new $2H_a$-MoS_2 structure [Fig. 1(b)] has at $p = 20$ GPa lattice parameters $a = 3.080$ Å, $c = 10.754$ Å with Mo atoms at Wyckoff position 2(b) and S atoms at 4(f) with $z = 0.8947$. As the band structures in Figs. 3(d) and 3(e) show, the new phase $2H_a$-MoS_2, also semiconducting at low pressures, undergoes a pressure-induced band overlap metallization now near 20 GPa. The Fermi surface of the $2H_a$ structure at 31 GPa shown in Fig. 3(f) is similar to that of the $2H_c$ phase, containing a hole pocket at Γ and electron pockets slightly further from the Γ point and closer to the K points of the BZ. The $2H_a$ structure is therefore also a candidate for the excitonic insulator with a slightly longer modulation wave vector compared to $2H_c$. Structurally, $2H_a$ is less anisotropic than the initial $2H_c$ structure, the new interlayer spacing (reflected in the c-axis length) smaller, the in-plane interatomic spacing (reflected by the a,b lengths) larger.

At this point comes an important contact with the experiment. A few years ago Aksoy *et al.*[10] reported an unspecified structural transformation taking place in $2H_c$-MoS_2 between 20 and 30 GPa, without change of space group symmetry. When we overlap their measured lattice parameters a and c with our calculated ones in Fig. 2 the conclusion that their observed transformation is precisely the $2H_c$ to $2H_a$ transition strongly suggests itself. To further nail down that conclusion we calculated x-ray powder patterns for $2H_c$-MoS_2 and $2H_a$-MoS_2 and compared them in Fig. 5 with the measured ones. Again, the agreement is quite good. The pressure-induced onset of the $2H_a$ phase is heralded by the birth of a (104) reflection (indexed as "006" in Ref. 10) and a much stronger (102) reflection. The simultaneous demise of the $2H_c$-MoS_2 phase is signaled by the disappearance of (105) and the drop of (103) reflections.

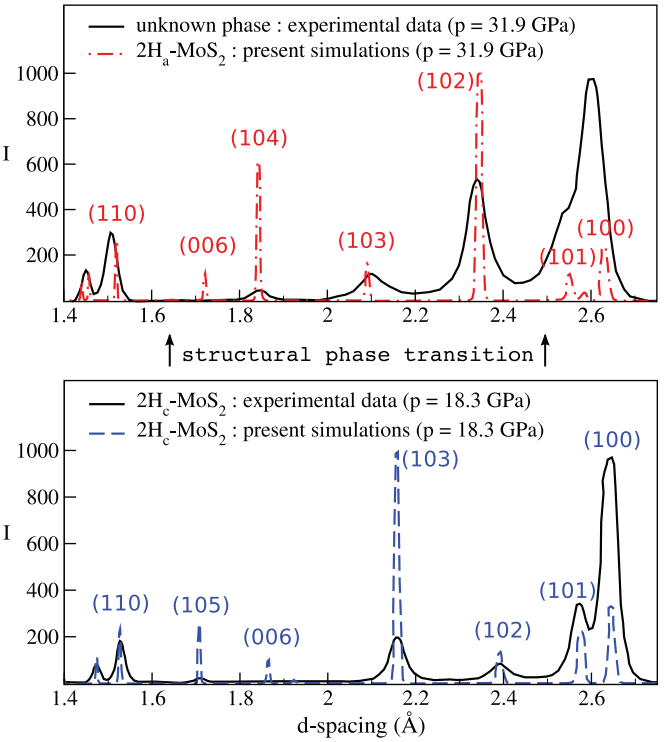

FIG. 5. (Color online) Comparison of experimental (Ref. 10) and calculated x-ray diffraction patterns for $2H_c$ structure below 20 GPa and $2H_a$ structure above 20 GPa.

Raman spectroscopy data[11] are also available for MoS_2 in the pressure interval up to 31 GPa. At $p = 19.1$ GPa a new peak (called "d" band, Figs. 5 and 6 in Ref. 11) appears, first as a shoulder on the high-frequency side of the original E_{2g} peak. As pressure grows its weight increases at the expense of the original E_{2g} peak and at 23.4 and 31 GPa both peaks are clearly visible in the spectra. Using the QUANTUM ESPRESSO code[32] we calculated the frequencies of Raman active E_{2g} and A_{1g} phonon modes of $2H_c$-MoS_2 and $2H_a$-MoS_2 at the same

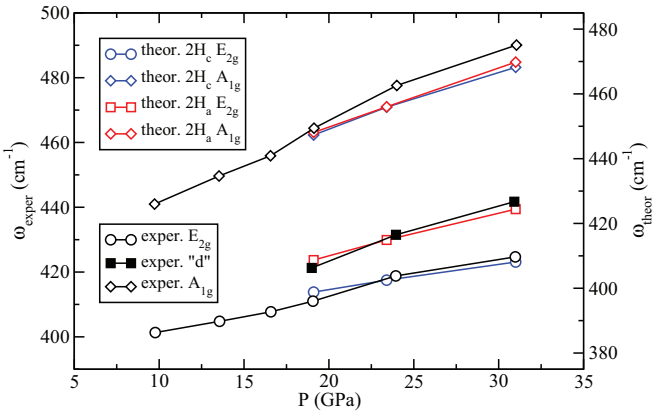

FIG. 6. (Color online) Comparison of experimental (Ref. 11) and calculated peak positions of Raman spectra for $2H_c$ and $2H_a$ structures at different pressures. The vertical axis for theoretical data (right) has been shifted with respect to the axis for experimental data (left) by 15 cm^{-1} upwards to account for a small constant difference between the two datasets.

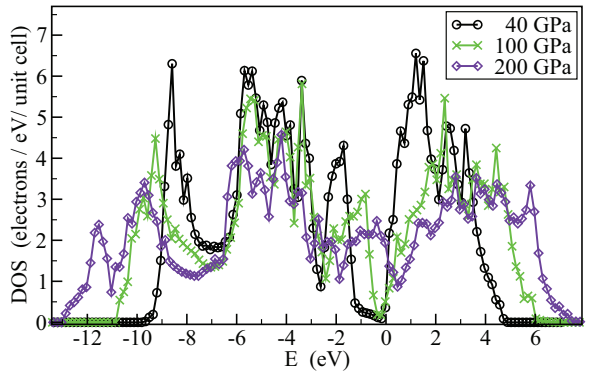

FIG. 7. (Color online) $2H_a$-MoS_2 electronic density of states at selected pressures.

experimental pressures of 19.1, 23.4, and 31 GPa (Ref. 34). A comparison with the experimental data[11] in Fig. 6 suggests that the "d" band coincides with the E_{2g} mode of the emergent $2H_a$ phase. On the other hand, the difference of frequency of the higher A_{1g} mode in both phases is very small, which explains why this peak is not observed to split in the experiment. Apart from a small systematic difference of about 15 cm^{-1} between the experimental and calculated peak positions the overall agreement is very good. This provides further strong support for the $2H_c \rightarrow 2H_a$ structural transition starting at 20 GPa with both phases coexisting up to the highest pressure of 31 GPa.

Since the experimental observations stop just below 40 GPa, we extended simulations to higher pressures to look out for further events and possible transformations.[35] At 120 GPa, searching for newer potential structural transitions, we carried out another metadynamics simulation, but the $2H_a$ structure within the 72-atom supercell remained stable and did not show any transition.

Finally, even at very high pressures, $2H_a$-MoS_2 remains essentially semimetallic as seen in the electronic density of states in Fig. 7. Poor metallicity is probably the reason why Raman spectra are still well defined even at 31 GPa. Using again the QUANTUM ESPRESSO code[32] we calculated the dimensionless electron-phonon coupling λ for both $2H_a$ and $2H_c$ phases and found it to be smaller than 0.12 for pressures up to 100 GPa. Thus, unlike the metal intercalated compounds, pristine $2H$-MoS_2 is not prone to superconductivity, at high pressures. If, on the other hand, charge or spin-density waves were to occur near the gap closing, these phases could be preceded or followed as a function of pressure by narrow superconducting regions at low temperatures.

IV. CONCLUSION

Our overall physical conclusions are that pressure will cause MoS_2 layers to slide, resulting in a structural transition between $2H_c$ and $2H_a$ polytypes, via a process akin to superlubric sliding.[33] In both structures, band overlap metallization should take place at relatively low pressures. After that, however, the broad cleft between valence and conduction bands, both with large Mo d-band character, does not shrink fast enough to produce a comparably large metallicity to that generated by, e.g., alkali doping, or by EDL field doping.[6,7] High pressure MoS_2 is predicted to remain semimetallic and not prone to superconductivity up to 100 GPa. The contrast with the higher superconducting temperatures obtained by alkali and by EDL electron doping stems first of all from the smaller density of states (DOS) achievable by pressure, but can also be related to a higher coupling of electrons relative to holes, and to a dimensionality effect in the EDL case. One aspect that remains to be explored is the possible occurrence, to be pursued with methods beyond those currently available, of excitonic insulator driven charge or spin-density waves in a narrow pressure range close to the metallization pressure. If such a phase did exist, it is likely to be preceded and/or followed by a superconducting region.

ACKNOWLEDGMENTS

E.T. thanks T. Kagayama, Y. Iwasa, A. Shukla, and M. Calandra for discussions and the exchange of information. Work in Trieste was partly sponsored by EU-Japan Project LEMSUPER, by Sinergia Contract No. CRSII2$_1$36287/1, and benefited from early advances on ERC Advanced Grant No. 320796—MODPHYSFRICT. L.H. and R.M. were supported by the Slovak Research and Development Agency under Contract No. APVV-0558-10 and by the project implementation 26220220004 within the Research & Development Operational Programme funded by the ERDF. Part of the calculations were performed in the Computing Centre of the Slovak Academy of Sciences using the supercomputing infrastructure acquired in project ITMS 26240120025 (Slovak infrastructure for high-performance computing) supported by the Research & Development Operational Programme funded by the ERDF. L.H. acknowledges a predoc fellowship held at SISSA during part of this project.

*martonak@fmph.uniba.sk

[1] L. Gmelin, in *Gmelin Handbook of Inorganic and Organometallic Chemistry*, Vol. B 7–9 (Springer-Verlag, Berlin, 1995), p. 16.
[2] M. Dallavalle, N. Sndig, and F. Zerbetto, Langmuir **28**, 7393 (2012).
[3] K. F. Mak, C. Lee, J. Hone, J. Shan, and T. F. Heinz, Phys. Rev. Lett. **105**, 136805 (2010).
[4] B. Radisavljevic, A. Radenovic, J. Brivio, V. Giacometti, and A. Kis, Nat. Nano. **6**, 147 (2011).
[5] R. B. Somoano, V. Hadek, and A. Rembaum, J. Chem. Phys. **58**, 697 (1973).
[6] K. Taniguchi, A. Matsumoto, H. Shimotani, and H. Takagi, Appl. Phys. Lett. **101**, 042603 (2012).
[7] J. T. Ye, Y. J. Zhang, R. Akashi, M. S. Bahramy, R. Arita, and Y. Iwasa, Science **338**, 1193 (2012).
[8] S. Bhattacharyya and A. K. Singh, Phys. Rev. B **86**, 075454 (2012).
[9] M. Dave, R. Vaidya, S. G. Patel, and A. R. Jani, Bull. Mater. Sci. **27**, 213 (2004).

[10]R. Aksoy, Y. Ma, E. Selvi, M. C. Chyu, A. Ertas, and A. White, J. Phys. Chem. Solids **67**, 1914 (2006).
[11]T. Livneh and E. Sterer, Phys. Rev. B **81**, 195209 (2010).
[12]R. Martoňák, A. Laio, and M. Parrinello, Phys. Rev. Lett. **90**, 075503 (2003).
[13]R. Martoňák, D. Donadio, A. R. Oganov, and M. Parrinello, Nat. Mater. **5**, 623 (2006).
[14]R. Martoňák, in *Modern Methods of Crystal Structure Prediction*, edited by A. R. Oganov (Wiley-VCH, Berlin, 2011).
[15]R. Martoňák, Eur. Phys. J. B **79**, 241 (2011).
[16]G. Kresse and J. Furthmüller, Phys. Rev. B **54**, 11169 (1996).
[17]G. Kresse and D. Joubert, Phys. Rev. B **59**, 1758 (1999).
[18]H. J. Monkhorst and J. D. Pack, Phys. Rev. B **13**, 5188 (1976).
[19]J. P. Perdew, K. Burke, and M. Ernzerhof, Phys. Rev. Lett. **77**, 3865 (1996).
[20]A. D. Becke, J. Chem. Phys. **98**, 5648 (1993).
[21]P. J. Stephens, F. J. Devlin, C. F. Chabalowski, and M. J. Frisch, J. Phys. Chem. **98**, 11623 (1994).
[22]A. V. Krukau, O. A. Vydrov, A. F. Izmaylov, and G. E. Scuseria, J. Chem. Phys. **125**, 224106 (2006).
[23]S. Grimme, J. Comput. Chem. **27**, 1787 (2006).
[24]The XCrySDen program (A. Kokalj, Comput. Mater. Sci. **28**, 155 (2003), http://www.xcrysden.org) was used to visualize the path in BZ in Fig. 1(c) and Fermi surfaces in Fig. 3(c,f).
[25]We adopt here the notation of Katzke *et al.* (Ref. 30), while in earlier works such as, e.g., Ref. 31, this structure was denoted as $2H_b$.
[26]H. Guo, T. Yang, P. Tao, Y. Wang, and Z. Zhang, J. Appl. Phys. **113**, 013709 (2013).
[27]H. Cercellier, C. Monney, F. Clerc, C. Battaglia, L. Despont, M. G. Garnier, H. Beck, P. Aebi, L. Patthey, H. Berger, and L. Forró, Phys. Rev. Lett. **99**, 146403 (2007).
[28]C. Monney, H. Cercellier, F. Clerc, C. Battaglia, E. F. Schwier, C. Didiot, M. G. Garnier, H. Beck, P. Aebi, H. Berger, L. Forró, and L. Patthey, Phys. Rev. B **79**, 045116 (2009).
[29]D. Jérome, T. M. Rice, and W. Kohn, Phys. Rev. **158**, 462 (1967).
[30]H. Katzke, P. Tolédano, and W. Depmeier, Phys. Rev. B **69**, 134111 (2004).
[31]F. E. Wickman and D. K. Smith, Am. Mineral. **55**, 1843 (1970).
[32]P. Giannozzi *et al.*, J. Phys.: Condens. Matter **21**, 395502 (2009).
[33]A. Vanossi, N. Manini, M. Urbakh, S. Zapperi, and E. Tosatti, Rev. Mod. Phys. **85**, 529 (2013).
[34]We used the PBE PAW pseudopotentials Mo.pbe-spn-kjpaw.UPF and S.pbe-n-kjpaw.UPF.
[35]Above 50 GPa we used the hard version of VASP PAW pseudopotentials.